

A Chandra Study: Are Dwarf Carbon Stars Spun Up and Rejuvenated by Mass Transfer?

PAUL J. GREEN,¹ RODOLFO MONTEZ,¹ FERNANDO MAZZONI,² JOSEPH FILIPPAZZO,³ SCOTT F. ANDERSON,⁴
ORSOLA DE MARCO,⁵ JEREMY J. DRAKE,¹ JAY FARIHI,⁶ ADAM FRANK,⁷ JOEL H. KASTNER,⁸ BRENT MISZALSKI,⁹ AND
BENJAMIN R. ROULSTON^{10,1}

¹Harvard Smithsonian Center for Astrophysics, 60 Garden St, Cambridge, MA 02138, USA

²University of Massachusetts, Lowell

³Space Telescope Science Institute 3700 San Martin Drive, Baltimore, MD 21218, USA

⁴Department of Astronomy, University of Washington, Box 351580, Seattle, WA 98195, USA

⁵Department of Physics & Astronomy, Macquarie University, Sydney, NSW 2109, Australia; Astronomy, Astrophysics and
Astrophotonics Research Centre, Macquarie University, Sydney, NSW 2109, Australia

⁶Department of Physics and Astronomy, University College London, WC1E 6BT, UK

⁷Department of Physics and Astronomy, University of Rochester, Rochester, NY 14627-0171, USA

⁸Chester F. Carlson Center for Imaging Science, Rochester Institute of Technology, 54 Lomb Memorial Drive, Rochester NY 14623 USA
; School of Physics & Astronomy and Laboratory for Multiwavelength Astrophysics, Rochester Institute of Technology, 54 Lomb
Memorial Drive, Rochester NY 14623 USA)

⁹South African Astronomical Observatory, PO Box 9, Observatory 7935, South Africa; Southern African Large Telescope Foundation, PO
Box 9, Observatory 7935, South Africa

¹⁰Department of Astronomy, Boston University, 725 Commonwealth Avenue, Boston, MA 02215, USA

(Received May 15, 2019; Revised June 20, 2019)

ABSTRACT

Carbon stars (with $C/O > 1$) were long assumed to all be giants, because only AGB stars dredge up significant carbon into their atmospheres. The case is nearly iron-clad now that the formerly mysterious dwarf carbon (dC) stars are actually far more common than C giants, and have accreted carbon-rich material from a former AGB companion, yielding a white dwarf and a dC star that has gained both significant mass and angular momentum. Some such dC systems have undergone a planetary nebula phase, and some may evolve to become CH, CEMP, or Ba giants. Recent studies indicate that most dCs are likely from older, metal-poor kinematic populations. Given the well-known anti-correlation of age and activity, dCs would not be expected to show significant X-ray emission related to coronal activity. However, accretion spin-up might be expected to rejuvenate magnetic dynamos in these post mass-transfer binary systems. We describe our *Chandra* pilot study of six dCs selected from the SDSS for $H\alpha$ emission and/or a hot white dwarf companion, to test whether their X-ray emission strength and spectral properties are consistent with a rejuvenated dynamo. We detect all 6 dCs in the sample, which have X-ray luminosities ranging from $\log L_x \sim 28.5 - 29.7$, preliminary evidence that dCs may be active at a level consistent with stars that have short rotation periods of several days or less. More definitive results require a sample of typical dCs with deeper X-ray observations to better constrain their plasma temperatures.

Keywords: binaries: general – stars: chemically peculiar – stars: carbon – X-rays: stars

1. INTRODUCTION

1.1. Dwarf Carbon Stars

Carbon (C) stars show molecular absorption bands of carbon — C_2 , CN or CH in their optical spectra — because they have $C/O > 1$, with atmospheres cool enough to form molecules. By contrast, the C/O ratio for nearby Sun-

like stars is between $\sim 0.5 - 0.8$ (Fortney 2012 and references therein). In most single stars of intermediate mass ($\sim 1 - 8 M_{\odot}$), atmospheres show C/O above unity only in the asymptotic giant branch phase, when carbon is brought to the surface during episodes of strong convection. The so-called third dredge-up occurs during late stages of thermal pulsations (the TP-AGB phase), associated with the triple- α process in shell He-burning episodes. AGB stars may reach a radius of ~ 1 A.U. ($\sim 200 R_{\odot}$). Pulsations, shocks and radiation all drive carbon- and s -process- enhanced material outward in an AGB wind, which may result in detached shells of circumstellar material containing 50 – 70% of the star’s mass (Wood et al. 2004). Winds from AGB stars are the predominant source of carbon in the interstellar medium, the PAHs in star-forming regions, pre-biotic molecules and indeed the planets as well (e.g., Tielens 2005).

The discovery of the first *main sequence* carbon star G77-61 ($M_V = 10.1$; Dahn et al. 1977) sounded like an oxymoron at the time. Dahn et al. (1977) offered several possible explanations for the existence of a dwarf carbon (dC) star. That G77-61 is in a binary system ($P \sim 245$ d; Dearborn et al. 1986) with an unseen companion consistent with a cool white dwarf, strongly suggested that extrinsic processes produce the dC’s enhanced atmospheric abundances. Recent results from radial velocity monitoring of larger samples of dCs are consistent with a 100% binary fraction (Whitehouse et al. 2018; Roulston et al. 2019). Therefore, the favored hypothesis to explain dCs is that C-rich material lost in an AGB wind can be efficiently captured by a main-sequence companion. While the AGB donor has since evolved to a white dwarf (WD), the “polluted” companion, as an innocent bystander, could be either dwarf or giant in the current epoch. Indeed, a variety of non-AGB stars, including many red giant stars, show enhanced carbon and/or s -process abundances that are similarly extrinsic. The CH, Ba and the carbon-enhanced metal poor (CEMP- s) stars (Lucatello et al. 2005) - mostly giants or subgiants - likely evolved from dC stars, and have been more commonly studied only by virtue of their greater brightness. All these objects can show atmospheric signatures of s -process elements associated with neutron capture onto iron seed nuclei in AGB stars.

Is there another viable path to strong carbon enhancement besides mass transfer? Intriguingly, the CEMP-no class lacks s -process overabundances, and initial radial velocity studies do not show an enhanced binary fraction (Starkenburg et al. 2014), so CEMP-no stars may achieve atmospheric carbon enhancement without mass transfer. Debate continues, but one suggestion is that (reminiscent of one of the suggestions in Dahn et al. 1977) CEMP-no stars may have coalesced from clouds seeded with strong carbon overabundances (and insignificant iron) by the first zero-heavy-element stars (e.g., Bromm, & Loeb 2003; Norris et al. 2013). This interpretation is favored by the fact that nearly all CEMP-no stars have $[\text{Fe}/\text{H}] \leq -4.0$. The prototype dC star, G77-61 has a companion, but also has extremely low metallicity ($[\text{Fe}/\text{H}] \sim -4$; Plez & Cohen 2005), so might be a candidate for either mechanism.

The importance of dC stars like G77-61 was later confirmed as many additional dCs were recognized from their large proper motions (Green et al. 1991; Downes et al. 2004). In a handful of cases, the “smoking gun” of AGB binary mass transfer was revealed as a hot DA white dwarf companion (Heber et al. 1993; Liebert et al. 1994). More recently Green (2013) found more than 700 dC stars in the SDSS, powerfully confirming that dCs are in fact the *numerically dominant* type of carbon star in the Galaxy, supporting the ubiquity of the dC phenomenon across a broad range of mass and age. Other large samples have since emerged from LAMOST (Ji et al. 2016; Li et al. 2018), including a dozen double-line spectroscopic binary (SB2) DA+dC spectra, which reveal recently-minted systems (Si et al. 2014). Dwarf carbon stars show kinematic evidence of mostly belonging to older populations (Green 2013; Farihi et al. 2018). Dwarf carbon stars may be favored in older e.g., thick disk or halo systems because they are born with large C/O (as for the CEMP-no hypothesis above) or simply because at lower metallicity, less mass transfer is required to boost $\text{C}/\text{O} > 1$.

Dozens of dCs show Balmer emission lines, signs of strong chromospheric activity. This is surprising, since activity is rare in older stars. Activity is also associated with enhanced X-ray emission, which for dC stars remains uncharacterized. Stellar activity - which correlates with rapid rotation in the general population (see § 1.4 below) - may be a result of spin-up by accretion in dC stars, a hypothesis we aim to test here via X-ray observations.

1.2. The Planetary Nebula Connection

Once the hot core of an AGB star is revealed, it may illuminate the layers of expelled material to form a spectacular planetary nebula (PN). Binary companions to the central stars of PNe (CSPNe) are widely believed to be responsible for bipolar (axisymmetric) structures in PNe (see, e.g., Balick & Frank 2002; Balick 2004; García-Segura et al. 2018). Many dC stars were likely born within planetary nebulae. Indeed, the CSPN of PN G054.2-03.4 (“The Necklace”; Miszalski, et al. 2013) reveals a dC spectrum when the CSPN is in eclipse, offering *direct* evidence for this link between PNe and dC stars.

Surviving main sequence companions to CSPNe may be “born-again” - resembling pre-main sequence stars, but with rejuvenated coronae and (hence) luminous X-ray emission (Soker & Kastner 2002). *Chandra* imaging of CSPNe (Montez, et al. 2010) has revealed that most of the pointlike X-ray sources are too hard to be modeled as blackbody emission from a pre-WD stellar photosphere ($\sim 100\text{--}200\text{kK}$). Among CSPNe with hard X-ray emission ($T_X \gtrsim 6\text{MK}$), at least 75% (6 out of 8) have known close or rapidly rotating companions (Kastner, et al. 2012; Montez et al. 2015). The companions are expected to remain active much longer ($> \text{Gyr}$; West et al. 2008) than characteristic PN lifetimes ($\sim 10^5 \text{yr}$; e.g., Frew 2008). While the nearest known binary CSPNe with hard X-rays are at $\sim 500 \text{pc}$ (NGC 1514 at $460 \pm 8 \text{pc}$ and LoTr 5 at $499 \pm 12 \text{pc}$; Bailer-Jones et al. 2018), field dCs are worthy of study because some are as close as $\sim 80 \text{pc}$, and uncontaminated in the X-rays by hot CSPN radiation.

1.3. Binary Evolution Scenarios

Mass transferred from the former AGB companion may occur via stellar wind, Roche-lobe overflow (RLOF), and/or common-envelope (CE) evolution. Models for dC formation in both the disk and halo (de Kool & Green 1995) predict a bimodal orbital period distribution, with a large peak near a decade, for objects that have accreted AGB wind material with no substantial decrease of the orbital separation. A smaller peak near 1 year likely contains systems that underwent a CE phase, where the companion was subsumed in the expanding atmosphere of the AGB star when it filled its Roche lobe. These models reproduce the well-studied distributions of CH and Ba II giants, whose progenitors are almost certainly the dC stars. However, many gaps remain in our understanding. For instance, using a variety of reasonable typical assumptions about the initial period distribution and the physics of the mass-transfer process, the synthetic populations of Abate et al. (2018) under-predict the frequency of short period systems relative to an unbiased sample of observed CEMP-*s* stars (e.g., Iaconi et al. 2018).

Very small initial orbital separations may not readily result in dC stars, because the primary will fill its Roche lobe, truncating evolution before the TP-AGB phase. However, orbits can evolve in a variety of ways as described e.g., by Chen et al. (2018). Recent results from radial velocity monitoring of dCs (Whitehouse et al. 2018; Roulston et al. 2019) find some dCs with unexpectedly short periods (1.2 days Corradi et al. 2011; Miszalski, et al. 2013; ~ 3 days; Margon et al. 2018) or show large RV variations with as-yet undetermined orbits (Roulston et al. 2019). The dCs may prove quite important for further studies, because we know directly from their C_2 and CN bands that they are post-AGB mass transfer binaries, which makes them especially valuable laboratories of stellar binary evolution.

1.4. Stellar Rotation and Activity

Since dC stars seem to be from older (thick disk or halo) populations (Green 2013; Farihi et al. 2018), their congenital rotation rates, dynamo strengths and related activity should have wound down significantly (e.g., Gondoin 2018 and references therein). However, Jeffries & Stevens (1996) describe how the accretion of a massive, slow (10 - 20 km/s) AGB wind is expected to spin up its low-mass secondary to short ($\lesssim 10 \text{hr}$) rotation periods, for final orbital separations of about 100 AU or less. We may therefore expect significant activity and X-ray emission to be characteristic of dC stars - at least those in similar orbits - even if their progenitors may be older than most active stars in the Galaxy.

The activity lifetimes inferred for M dwarfs range from $\sim 1 - 5 \text{Gyr}$ (for M1 - M4 stars; West et al. 2008). The dC stars could remain active for similar timespans after mass transfer. The active fraction among late-type stars as a function of age, metallicity and binary orbital elements is a current topic of strong interest (e.g., West et al. 2008; Morgan et al. 2012), but the strength, frequency or duration of activity in *rejuvenated* (post mass transfer) dwarfs remains unknown. The dC stars offer a unique tracer, because even without measured orbital signatures of binarity, their C_2 and CN bands mark them clearly as post mass transfer systems.

Depending on the host system metallicity and evolution, a dC star may have inherited a substantial fraction of its final mass by accretion (e.g., Miszalski, et al. 2013), potentially changing its overall structure in the process. Assuming the accreting star is fully convective, then it must inherit $0.1 - 0.2 M_\odot$ of C/O $\sim 2\text{--}3$ material. By contrast a much smaller quantity of more highly-enriched (e.g., C/O > 20) material would suffice. As mentioned above, the metallicity of the accretor is also key; for a star like G77-61 with extremely low metallicity (Plez & Cohen 2005), much less mass transfer is required from a donor with the same C/O.

After a major mass accretion event, the dwarf’s radius may remain inflated by accretion shocks, or even by enhanced magnetic activity itself, as debated for CSPNe (e.g., Jones et al. 2015). Nevertheless, long after the newly-minted dC settles back to the main sequence from a thermally unstable phase (with radius potentially $\sim 2.5\times$ greater than a normal dC; Afşar & Ibanoglu 2008), we expect a long-lasting ($\sim \text{Gyrs}$) active phase as the compact core cools and fades.

Rapid rotation rates are typically found in young stars, as long as they retain angular momentum from their initial collapse. Rapid rotation together with convection is thought to drive an internal magnetic dynamo and consequent magnetic activity (e.g., [Kosovichev et al. 2013](#) and references therein). The tangling, breaking and reconnection of magnetic field lines, as seen in the Sun, in turn generates chromospheric activity (associated observationally e.g., with H α emission) and coronal activity (associated with X-ray emission). These tracers of magnetic activity decrease with stellar rotation rates (e.g., [Pallavicini et al. 1981](#); [Reiners et al. 2012](#); [Wright et al. 2011](#)). Rotation periods of main sequence stars with outer convection zones increase with age due to angular momentum loss through magnetized winds (e.g., [Kraft 1967](#); [Matt et al. 2015](#); [Garraffo et al. 2018](#)).

Even though we do not yet have rotation periods measured for dCs, the detection of enhanced X-ray emission would provide very suggestive evidence that they have active dynamos, consistent with rotation rates enhanced by spin up from the accretion of angular momentum during past episodes of post-AGB binary mass transfer. This possibility motivated the pilot *Chandra* X-ray study whose results we describe below.

2. SAMPLE SELECTION

The list of six targets for this initial *Chandra* study of X-rays from dC stars was compiled from our uniformly-selected SDSS sample of high latitude C stars ([Green 2013](#)). We selected only those that are definitively main sequence, based on high proper motions measured between USNO-B and SDSS ([Munn et al. 2004](#)). (Any giant with such high proper motion would be nearby and much too bright for SDSS.) For the most resource-efficient exploration of dC stars, we restricted the sample to either DA+dC systems or dCs showing H α emission (dCe stars, henceforth) with $i < 17$, yielding 6 objects (2 DA+dCs, and 4 dCes). One was already observed in X-rays; SDSS J125017.90+252427.6 falls serendipitously in both XMM-*Newton* and *Chandra* fields ([Green 2013](#)), as it is only about 6 arcmin away from the galaxy NGC 4725.

The small pilot sample we consider here likely includes dC stars (1) with a relatively short time since accretion (the dC systems including still-hot DA white dwarfs) and/or (2) those still showing clear signs of activity (the dCe stars, for which the presumed DA white dwarf has cooled beyond detectability even in the optical/UV). SDSS spectra are shown in Fig 1 for the objects in our *Chandra* sample, illustrating the range of dC types herein.

For context, we make use of the distance information derived from Gaia Data Release 2 ([Gaia Collaboration et al. 2018](#)) by [Bailer-Jones et al. \(2018\)](#) to plot the range of color and absolute magnitude for a compilation of non-AGB carbon-enhanced stars in Fig 2. While originally selected based on their large proper motions, the dC systems in our sample are confirmed as definitively main sequence, having $M_G > 8$.

3. X-RAY OBSERVATIONS AND ANALYSIS

Our targeted *Chandra* observations of dC stars were performed using the S3 (backside illuminated CCD) on ACIS-S between 2014 October and 2016 May (proposals 15200243 and 16200105; P. Green P.I.). Exposure times ranged from 16 to 28 ksec per star. Some of the observations were split into several exposures (ObsIDs) as part of the requirement to keep various *Chandra* subsystem temperatures within their acceptable ranges. None of the observations uses a grating. Most are in VFAINT ACIS mode, but several are in FAINT mode; observation details are listed in Table 1.

For SDSS J163718.64+274026.5, we analyzed the merged observations, since they use the same instrument, and are only separated by two days (and just 4° in roll angle). SDSS J125017.90+252427.6 falls within 3 archival observations, with significantly different dates and instrument configurations, so we chose to analyze the longest observation only (29.6 ksec; PI Garmire).

We reprocessed the *Chandra* event lists with the CIAO (ver 4.10) `chandra_repro` script and CALDB (4.7.8), which account for afterglows, bad pixels, charge transfer inefficiency, and time-dependent gain corrections. All our dCs were detected in every *Chandra* ObsID, at positions within 2'' of those measured in Gaia DR2 (epoch 2015.5). We used the CIAO `srcflux` tool to estimate source properties in the 0.3-3.0 keV energy range, which includes all detected photons. X-ray source properties are shown in Table 3. To estimate intervening absorption from extinction due to Milky Way dust, we used the `dustmaps` Python package (Bayestar17) of ([Green 2018a](#)); for every dC direction, these columns were inconsequential.

For each dC, we derived two X-ray flux estimates, based on either a 2 MK or a 10 MK optically-thin plasma (APEC; [Smith, R.K. et al. 2001](#)) with absorption modeled using WABS ([Morrison & McCammon 1983](#)). As described in § A, our motivation for these choices comes both from the literature, and from attempts to fit the *Chandra* spectra of the

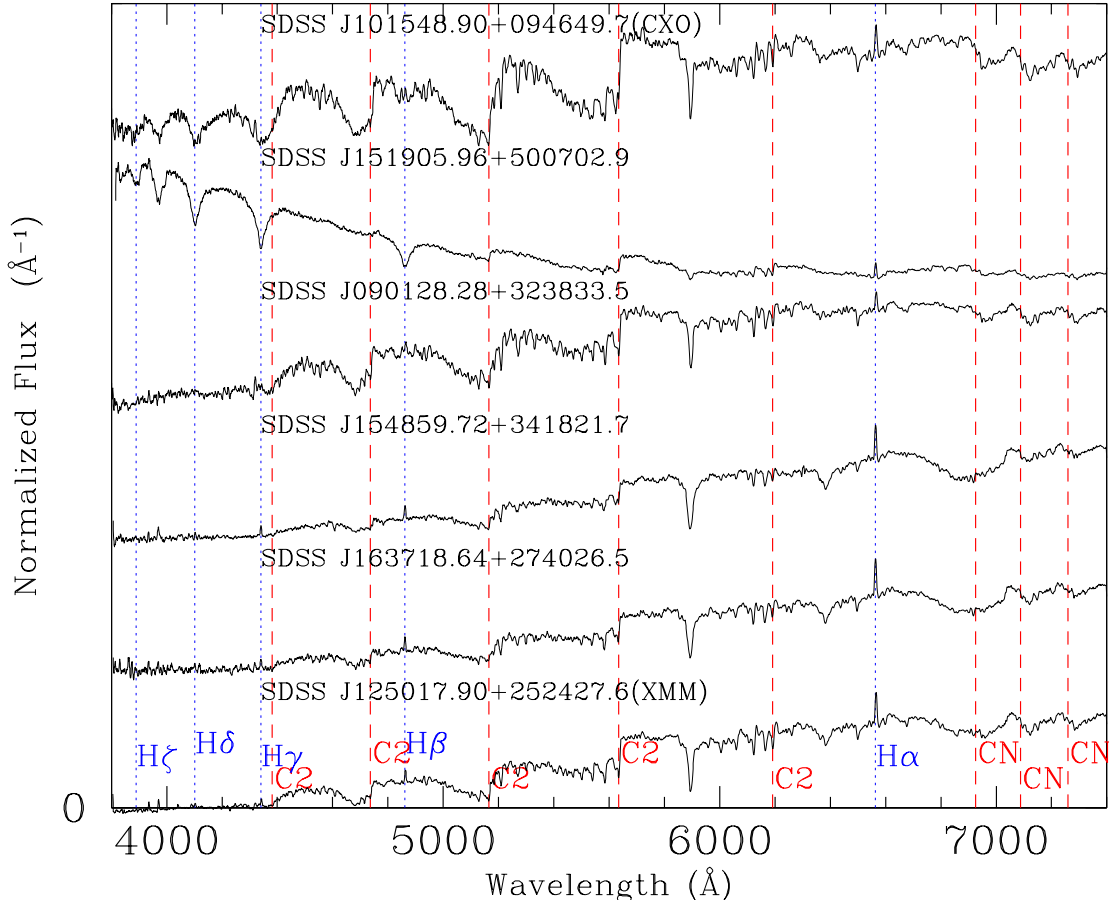


Figure 1. SDSS spectra of our full dC star sample. All show strong C₂ bands at λ 4737, 5165, and 5636, as well as H α emission betraying chromospheric activity. Broad Balmer absorption lines in the top 2 spectra reveal their hot white dwarf companions. C₂ bandhead positions are shown with red long-dashed lines, and Balmer line wavelengths with blue short-dashed lines.

two dCs herein with the most counts. Further discussion of our sample below includes results assuming either 2 or 10 MK plasma temperatures.

Our X-ray analysis is very unlikely to be complicated by emission from the white dwarfs, even in the DA+dC systems, because hot white dwarf photospheric X-ray emission is extremely soft. For white dwarfs in the field, emission of hard X-rays is almost always attributed to coronal emission from a late-type dwarf companion (O’Dwyer, et al. 2003). Indeed, among the thousands of WDs that have been observed (mostly serendipitously) by XMM-Newton or ROSAT, only a handful of single WDs have spectra that are hard like the CSPN (Bilíková et al. 2010). The great majority of the CSPNe with hard X-ray emission that do not have an easily-detected late-type companion may have e.g., an accreting white dwarf companion (Miszalski et al. 2019).

Hydrogen Balmer line emission from the stellar chromosphere is a known tracer of activity; H α line luminosity is well-correlated with projected rotation velocity $v \sin i$ (e.g., Maldonado et al. 2017 for M0 - M4 dwarfs) after excluding spectroscopic binaries. While all of the dCs in our sample have H α emission evident by selection, we are unable to reliably use the H α equivalent widths in these dCs to predict their X-ray emission. H α equivalent widths are not a suitable indicator of stellar activity and must be transformed into H α fluxes, as found by multiple studies (Reiners et al. 2012; Maldonado et al. 2017), before fitting H α - X-ray relations. However the correlation between H α flux and X-ray flux appears to be a weak one even in K and M dwarfs, and becomes only more problematic with dCs given the lack

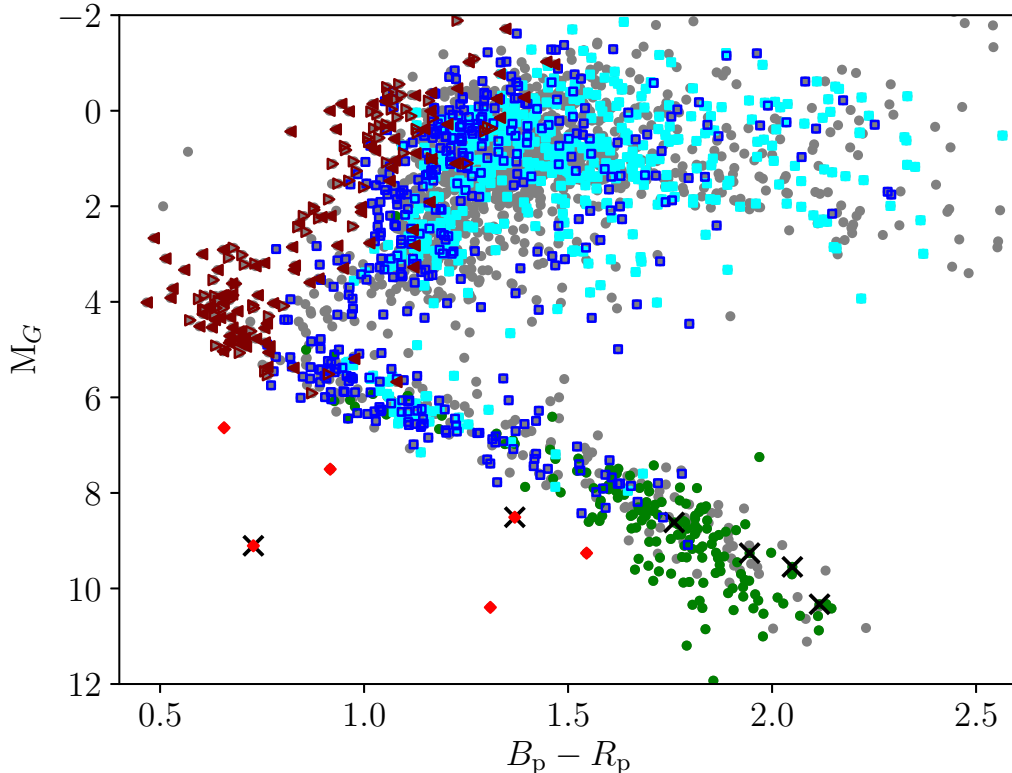


Figure 2. A color-magnitude diagram derived from our compilation of the latest spectroscopic samples of carbon-enhanced stars, using Gaia DR2 to derive an absolute G -band magnitude, and showing only significant parallaxes, with $\varpi/\sigma_\varpi > 5$. Dwarf carbon (dC) stars, largely from SDSS (Green 2013; Si et al. 2014) and LAMOST (Yoon et al. 2016; Li et al. 2018) form the main sequence, ($6 \lesssim M_G \lesssim 11$), most showing strong C_2 and CN molecular bands. Dwarfs identified in Green (2013) are shown by filled green circles. Red diamonds mark known DA/dC systems. The dCs observed with *Chandra* and analyzed herein are marked with large black crosses. CH (empty blue squares) and Ba II (filled cyan squares) from Li et al. (2018), and CEMP stars (maroon triangles) from Yoon et al. (2016) are also shown. As innocent bystanders to mass transfer, dCs are seen across a range of absolute magnitudes and temperatures, as long as they remain cool enough for C_2 and/or CN molecules to form (Green 2013). Most of the CH, Ba and CEMP stars are brighter than the turnoff ($M_G < 5$), and may well be evolved dC stars. We have not corrected for reddening on this plot; interstellar reddening is insignificant for most dCs. However, the reddest giants ($B_p - R_p \gtrsim 1.8$) are at low galactic latitude, and likely significantly reddened. A cross-correlation with the *Chandra* CSC2.0 (Evans et al. 2010) and XMM-Newton 3XMM-DR8 (Rosen et al. 2016) catalogs reveals no new matches among these stars.

of published model atmospheres needed to transform $H\alpha$ equivalent width into $H\alpha$ flux. We therefore did not attempt to use the observed $H\alpha$ emission to predict X-ray fluxes.

4. BOLOMETRIC LUMINOSITIES

Bolometric luminosity estimates are important for placing dCs in the context of other active stars, because stellar activity is best characterized in the X-rays across a range of stellar types when the X-ray luminosity is normalized by the bolometric luminosity and L_{bol} can vary by a factor of ~ 20 across the range of main sequence spectral types known to show C_2 and CN molecular bands. To estimate bolometric luminosities L_{bol} , we assembled a spectral energy distribution (SED) for each dC star in our sample from public cataloged photometry and calculated L_{bol} using the *sedkit* Python package (Filippazzo et al. 2015, Filippazzo et al., in prep). The exact procedure is detailed in those works and summarized here.

Optical, near-infrared, and mid-infrared magnitudes were obtained from the SDSS Data Release 12 (Alam et al. 2015), 2MASS Point Source Catalog (Skrutskie et al. 2006), and AllWISE Source Catalog (Cutri et al. 2013), respectively. We converted photometry to the VegaMag system and corrected for (small) interstellar extinction using the

Table 1. *Chandra* X-ray Observations

Object	Type	ObsID	Obs-Date	Exposure (ksec)	Inst.	Mode
SDSS J090128.28+323833.5	dCe	16650	2015-12-12	18.3	ACIS-S	VF
SDSS J101548.90+094649.7	DA/dC	15702	2015-01-18	15.9	ACIS-S	F
SDSS J125017.9+252427.6	dCe	409	1999-12-20	17.5	ACIS-S	F
		2976	2002-12-02	24.6	ACIS-S	F
		17461	2016-05-09	29.5	ACIS-I	VF
SDSS J151905.90+500702.9	DA/dC	16649	2016-05-16	27.6	ACIS-S	VF
SDSS J154859.72+341821.7	dCe	16651	2015-06-17	16.0	ACIS-S	VF
SDSS J163718.64+274026.5	dCe	17534	2014-10-19	8.5	ACIS-S	VF
		16652	2014-11-21	17.2	ACIS-S	VF

Table 2. Parallaxes, Distances and Bolometric Luminosities

Object	ϖ (mas)	Distance (pc)	$\log(L_{\text{bol}}/L_{\odot})$ erg/s
J0901	1.71 ± 0.14	577.1 ± 46.5	-1.26 ± 0.07
J1015	2.10 ± 0.13	469.9 ± 28.6	-1.32 ± 0.05
J1250	3.54 ± 0.08	280.6 ± 6.3	-1.52 ± 0.02
J1519	2.26 ± 0.08	438.0 ± 15.0	-1.47 ± 0.03
J1548	4.32 ± 0.08	229.9 ± 4.3	-1.87 ± 0.07
J1637	2.47 ± 0.09	401.6 ± 15.1	-1.56 ± 0.03

`dustmaps` Python package (Green 2018a). Synthetic magnitudes were calculated from the SDSS spectrum, which was then normalized to the observational photometry. In wavelength regions with no spectral coverage, the SED was linearly interpolated between photometric points. For the DA/dCs, we excluded the SDSS u , g and r band photometry and spectral flux, since they are contaminated by the DA white dwarfs. To approximate a Wien tail, the SED was linearly interpolated from the shortest wavelength data point down to zero flux at zero wavelength. A blackbody spectrum fit to the WISE photometry was used to approximate a Rayleigh-Jeans tail at long wavelengths. We then calculated the bolometric flux f_{bol} as the integral of the complete SED.

Finally, we calculated $L_{\text{bol}} = 4\pi f_{\text{bol}} d^2$ for each source using a parallax measurement from the Gaia DR2 and the resulting distances from Bailer-Jones et al. (2018). The results are shown in Table 2, where we adopt the solar bolometric luminosity value of $\log L_{\odot} = 33.583$.

5. ROTATION-ACTIVITY RELATIONSHIP

Field main sequence stars with outer convection zones are magnetically active, as traced by coronal X-rays and/or chromospheric H α emission. The large observed range in $\log L_x/L_{\text{bol}}$ from about 10^{-3} down to 10^{-8} , is thought to occur because stars' rotation rates slow with age, due to mass loss from stellar winds (e.g., Skumanich 1972). Indeed, rotation rates correlate strongly with activity, especially when normalized by the convective turnover time τ via the Rossby number $R_0 = P_{\text{rot}}/\tau$ (Noyes et al. 1984). The magnetic dynamo that drives these signatures of activity is thought to be generated by differential rotation inside the star. At the highest rotation rates, corresponding to $R_0 \lesssim 0.13$, activity saturates, and $\log L_x/L_{\text{bol}}$ remains at ~ -3.3 (Micela et al. 1985; Wright et al. 2011). It was long thought that this correlation must be mediated by an $\alpha\Omega$ dynamo (Parker 1955), which requires an interface (the

tachocline) between a solidly rotating radiative core, and a differentially rotating convective envelope. However, the same rotation-activity relationship appears to hold even for late-type stars thought to be fully convective (Wright et al. 2018).

Unfortunately, we do not have the sensitive multi-epoch photometry that would be required to measure the rotation rate for the dC stars in our sample. The greatest promise to achieve this in the near future - at least for the brighter dC examples - is after NASA's Transiting Exoplanet Survey Satellite (TESS) satellite (Ricker et al. 2015) surveys the northern sky, providing photometric measurements every 30 minutes, which can be combined as needed for greater sensitivity (at the cost of lower time resolution). Neither do we have estimates for the convective turnover times, due to a paucity of stellar structure models for dC stars. However, since we have empirical measurements of both L_x and L_{bol} , we can estimate the range of likely values of P_{rot} or R_0 for dC stars, reasonably assuming that their internal dynamics and magnetic dynamo have stabilized since the end of mass transfer.

In Fig 3, We show the activity level of dC stars in our sample as a function of rotation period, in context with activity in normal (C/O < 1) main sequence stars from several recent sources in the literature. Wright et al. (2018) studied the coronal activity-rotation relationship for late-type stars with rotation periods known from the MEarth project (Nutzman & Charbonneau 2008), including main sequence stars thought to be fully convective - those later than about M3 ($T_{\text{eff}} \lesssim 3300\text{K}$), corresponding to masses below about $\sim 0.35M_{\odot}$ (Chabrier & Baraffe 1997). Stelzer et al. (2016) compiled X-ray data from ROSAT and XMM-Newton catalogs for K2 Superblink stars with well-measured periods. They assumed a thermal (APEC) single temperature model (APEC) of 3.5MK and a column density of 10^{19} atoms cm^{-2} .

From Fig 3, limits on the rotational periods for these dC stars appear to be in the 'saturated' regime where $\log L_x/L_{\text{bol}} \geq -3.3$, at least when assuming plasma temperatures of $\sim 2\text{MK}$. About half remain in the saturated regime even when assuming a high plasma temperature $\sim 10\text{MK}$. If the lower temperature applies, then dCs' strong X-ray activity is consistent with rapid rotation rates of several days or less, as might be expected from accretion spin-up. If the higher temperature applies, then periods are more weakly constrained, to about 20 days or less.

Table 3. X-ray Source Properties in the 0.3-3.0 keV Energy Range

Object	Chandra	Net CR	T_X	$F_{X,\text{obs}}$	F_X	L_X
	ObsID	(cnt ks^{-1})	(MK)	10^{-15} erg cm^{-2} s^{-1})		(10^{28} erg s^{-1})
J0901	16650	0.16 ± 0.09	2	$3.18^{+4.33}_{-2.25}$	$3.77^{+5.14}_{-2.67}$	$15.47^{+21.12}_{-11.02}$
...	10	$0.97^{+1.33}_{-0.69}$	$1.03^{+1.41}_{-0.73}$	$4.23^{+5.79}_{-3.01}$
J1015	15702	0.25 ± 0.13	2	$3.64^{+4.00}_{-2.30}$	$4.82^{+5.28}_{-3.04}$	$13.02^{+14.28}_{-8.25}$
...	10	$1.34^{+1.48}_{-0.85}$	$1.48^{+1.63}_{-0.93}$	$4.00^{+4.41}_{-2.53}$
J1250	409	1.62 ± 0.99	2	$20.40^{+29.00}_{-15.08}$	$22.90^{+32.50}_{-16.93}$	$21.91^{+31.09}_{-16.20}$
...	10	$8.48^{+12.02}_{-6.27}$	$8.83^{+12.57}_{-6.53}$	$8.45^{+12.03}_{-6.25}$
...	2976	0.64 ± 0.17	2	$12.80^{+6.50}_{-5.00}$	$14.40^{+7.30}_{-5.64}$	$13.78^{+6.99}_{-5.40}$
...	10	$4.13^{+2.11}_{-1.61}$	$4.31^{+2.19}_{-1.68}$	$4.12^{+2.10}_{-1.61}$
...	17461	0.41 ± 0.12	2	$47.30^{+27.00}_{-19.70}$	$53.10^{+30.30}_{-22.10}$	$50.80^{+29.01}_{-21.17}$
...	10	$6.03^{+3.45}_{-2.51}$	$6.28^{+3.59}_{-2.62}$	$6.01^{+3.44}_{-2.51}$
J1519	16649	0.54 ± 0.14	2	$12.80^{+6.30}_{-4.77}$	$14.40^{+7.10}_{-5.39}$	$33.83^{+16.72}_{-12.72}$
...	10	$3.52^{+1.75}_{-1.31}$	$3.67^{+1.81}_{-1.37}$	$8.62^{+4.26}_{-3.23}$
J1548	16651	0.31 ± 0.14	2	$5.35^{+5.15}_{-3.14}$	$6.00^{+5.80}_{-3.52}$	$3.84^{+3.71}_{-2.25}$
...	10	$0.26^{+1.06}_{-0.26}$	$0.27^{+1.10}_{-0.27}$	$0.17^{+0.70}_{-0.17}$
J1637	16652	0.57 ± 0.18	2	$7.90^{+5.00}_{-3.49}$	$11.00^{+7.00}_{-4.85}$	$21.65^{+13.80}_{-9.58}$
...	10	$3.03^{+1.91}_{-1.34}$	$3.40^{+2.15}_{-1.50}$	$6.69^{+4.24}_{-2.96}$
...	17534	1.05 ± 0.35	2	$14.20^{+9.50}_{-6.59}$	$19.80^{+13.20}_{-9.20}$	$38.97^{+26.02}_{-18.16}$
...	10	$5.50^{+3.68}_{-2.55}$	$6.18^{+4.12}_{-2.86}$	$12.16^{+8.12}_{-5.65}$

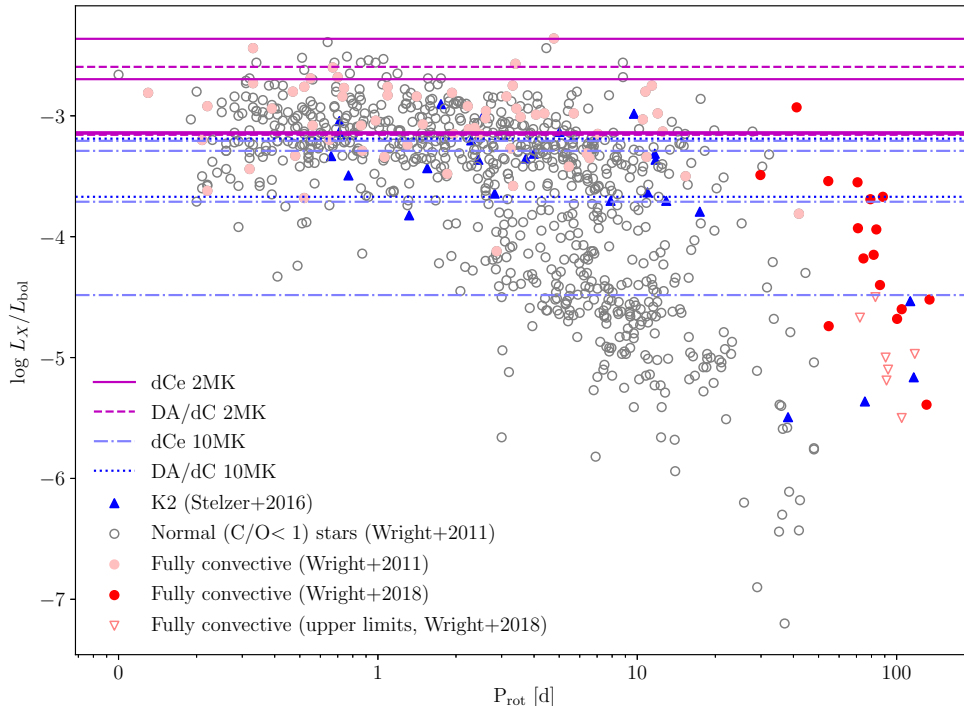


Figure 3. The activity level of dC stars in our sample in context with activity in normal ($C/O < 1$) main sequence stars. The logarithm of X-ray to bolometric luminosity ratio $\log L_x/L_{\text{bol}}$ is plotted vs. rotation period for the normal dwarf stars in the sample of Wright et al. (2011) (open black circles). Fully convective dwarfs are highlighted from Wright et al. (2018) (red circles, or red triangles for the upper limits) and from Wright et al. (2011) (faint red circles). Stars from the Kepler Two-Wheel (K2) samples of Stelzer et al. (2016) are shown as blue triangles. The horizontal magenta (blue) lines show the $\log L_x/L_{\text{bol}}$ values for the 6 dC stars observed by *Chandra* in our pilot program, assuming a plasma temperature of $T_X = 2MK$ ($T_X = 10MK$). Dashed (dotted) lines represent the 2 DA/dC systems (with a hot white dwarf still visible in the optical spectrum). Solid (dot-dash) lines are for the other dC systems.

We reiterate the caveats that (a) this pilot sample is not representative of dCs more generally since as mentioned, all 6 dC optical spectra in our sample show weak $H\alpha$ emission lines (see Fig 1) and (b) X-ray counts are too few to actually constrain T_X .

6. SUMMARY

We have sought to test the hypothesis that dC stars, having inherited significant mass from an extinct AGB companion, could have spun up significantly, and that they may therefore show signs of coronal activity often associated with rapid rotation. As a test for such coronal activity, we selected a small sample of dCs for X-ray observation with *Chandra*. All 6 dC systems observed were detected by *Chandra*, but with too few counts to allow useful spectral constraints. We therefore calculate X-ray fluxes assuming plasma temperatures of 2MK and 10MK, bracketing a range of reasonable values. We have estimated the dCs' bolometric luminosities directly by compiling and integrating multi-wavelength photometry, and using distances from Gaia DR2 parallaxes published after our *Chandra* observations were performed. When assuming a reasonable plasma temperature of 2MK, all 6 systems appear to have $\log L_x/L_{\text{bol}} \gtrsim -3$, putting them in the saturated regime so that they might be expected to have short ($\lesssim 10$ d) rotation periods consistent with strong accretion spin-up. At the upper range of expected temperature, near 10MK, the X-ray activity of dCs could imply longer ($\lesssim 20$ d) periods similar to less active dwarfs.

The X-ray emission from dC stars to date supports the mass transfer hypothesis. Where dCs have been part of a central binary system of a PN, which could be common, then the activity we detect here argues for spin-down

significantly longer than ($\sim 10^4$ year) PN timescales, because for most dC stars the former CSPNe are now WDs cooled beyond detectability.

To better understand the characteristics of a more typical sample, sufficiently sensitive X-ray observations of the closest known dC stars with reliable distances from Gaia DR2 are critical. Ideally, at least ~ 100 counts per object should be obtained, sufficient to constrain individual plasma temperatures to within about $\sim 30\%$. The X-ray luminosity fractions L_x/L_{bol} can then serve as a more reliable proxy to measure rotation and total accretion, within the context of models predicting longevity and intensity of the binary interaction during the AGB phase. For instance, accretion of both mass and angular momentum is enhanced if there is a longer RLOF phase before the CE phase. A dC enriched by a prolonged period of RLOF would have relatively stronger X-ray emission, faster rotation, and perhaps also higher C/O. Very close PCEB dC systems that have low X-ray activity may indicate a brief pre-CE phase. A dC that experienced only wind accretion may have low rotation and low L_x . A significant sample of dCs with measured orbital and rotation periods and X-ray luminosities would greatly enhance our understanding of these useful and intriguing systems.

The scientific results reported in this article are based on observations made by the *Chandra* X-ray Observatory, and data obtained from the *Chandra* Data Archive. This research has made use of software provided by the *Chandra* X-ray Center (CXC) in the application packages CIAO and Sherpa.

Support for this work was provided by the National Aeronautics and Space Administration through Chandra Award Numbers GO4-15005X and GO5-16004X issued by the Chandra X-ray Center, which is operated by the Smithsonian Astrophysical Observatory for and on behalf of the National Aeronautics Space Administration under contract NAS8-03060. BM acknowledges support from the National Research Foundation (NRF) of South Africa.

Funding for the Sloan Digital Sky Survey IV has been provided by the Alfred P. Sloan Foundation, the U.S. Department of Energy Office of Science, and the Participating Institutions. SDSS acknowledges support and resources from the Center for High-Performance Computing at the University of Utah. The SDSS web site is www.sdss.org.

SDSS is managed by the Astrophysical Research Consortium for the Participating Institutions of the SDSS Collaboration including the Brazilian Participation Group, the Carnegie Institution for Science, Carnegie Mellon University, the Chilean Participation Group, the French Participation Group, Harvard-Smithsonian Center for Astrophysics, Instituto de Astrofísica de Canarias, The Johns Hopkins University, Kavli Institute for the Physics and Mathematics of the Universe (IPMU) / University of Tokyo, Lawrence Berkeley National Laboratory, Leibniz Institut für Astrophysik Potsdam (AIP), Max-Planck-Institut für Astronomie (MPIA Heidelberg), Max-Planck-Institut für Astrophysik (MPA Garching), Max-Planck-Institut für Extraterrestrische Physik (MPE), National Astronomical Observatories of China, New Mexico State University, New York University, University of Notre Dame, Observatório Nacional / MCTI, The Ohio State University, Pennsylvania State University, Shanghai Astronomical Observatory, United Kingdom Participation Group, Universidad Nacional Autónoma de México, University of Arizona, University of Colorado Boulder, University of Oxford, University of Portsmouth, University of Utah, University of Virginia, University of Washington, University of Wisconsin, Vanderbilt University, and Yale University.

Facility: 2MASS, CXO, Gaia, Sloan, WISE

Software: `Astropy` (Astropy Collaboration et al. 2018), `matplotlib` (Barrett et al. 2005), `Numpy` (Oliphant 2006)

APPENDIX

A. X-RAY SPECTRAL MODELS

Our motivation for using 2MK and 10MK plasma temperatures for the X-ray spectral models of dC stars comes both from the literature and from our *Chandra* observations. The higher temperature model is consistent with median photon energies of $\sim 0.5 - 1.0$ keV (6 - 12 MK) seen in X-ray selected stellar samples observed with *Chandra* from e.g., the COSMOS survey (Wright et al. 2010), and also with the temperature of peak emissivity for Mg XI. However, for some single stars with detailed X-ray spectral fitting, plasma temperatures are close to 2 MK (e.g., see the compilation in Table 9 of Testa et al. 2004), the temperature of peak emissivity for O VII.

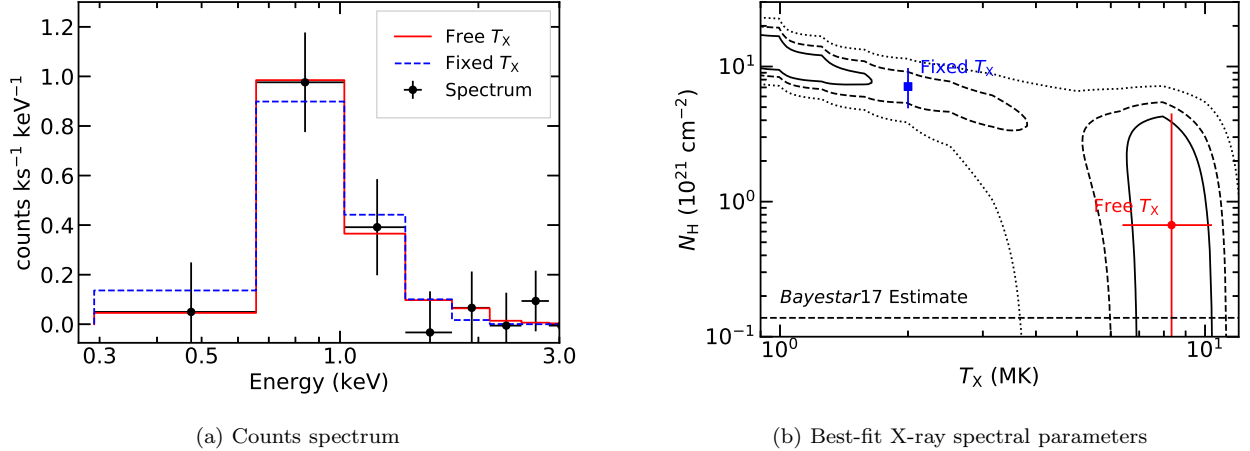
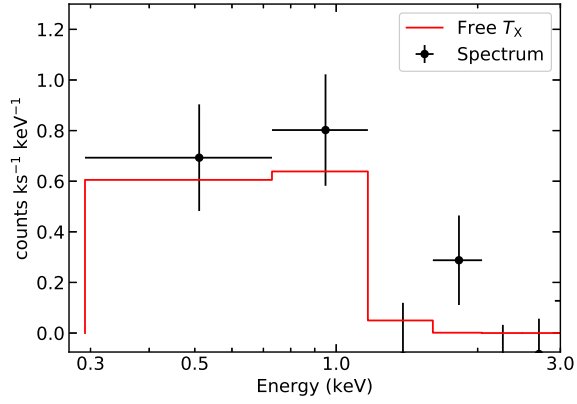


Figure 4. *Chandra* spectrum of SDSS J151905.90+500702.9 from ObsID 16649. (a) The photon spectrum in counts $\text{ksec}^{-1} \text{keV}^{-1}$. The expected counts for both 2 MK and 8 MK temperature plasma models are overplotted as blue dashed and red solid lines, respectively. Since the total number of net counts is only ~ 15 , the fits are equally good, and quite poorly constrained. (b) The best-fit contours (at 68.3, 90, and 99%) for the APEC spectral fit parameters of temperature T_X and intervening hydrogen column N_H . The intervening column estimated from Green (*Bayestar17*; 2018a) is quite low (dashed horizontal line), and is consistent with the best-fit spectrum for plasma temperature near ~ 8 MK. If we fix the temperature at $T_X = 2$ MK, a larger column is required, which may be consistent with possible circumstellar material.

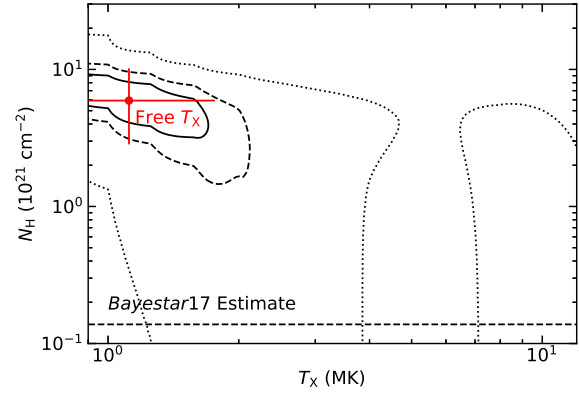
Even with very few counts detected in our *Chandra* images, we can examine the median energy values and their location with respect to the thermal models and foreground extinction. Most of the observed counts suggest $T_X > 3$ MK and likely near 8–10 MK, but this is uncertain without knowing what the circumstellar environment might contribute to extinction.

We can also analyze the two dCs in our sample with the largest number of counts, which are nonetheless insufficient for strong spectral model constraints. SDSS J151905.90+500702.9 (Fig 4) indicates that either a hot plasma temperature (~ 10 MK with low absorbing column, $N_H < 5 \times 10^{21} \text{ cm}^{-2}$) or a cool plasma temperature ($\lesssim 2$ MK, with high absorbing column, $N_H > 5 \times 10^{21} \text{ cm}^{-2}$) might be applicable. The best-fit spectral model for SDSS J125017.9+252427.6 (Fig 5) is single-peaked towards a cool value near ~ 1 MK.

These crude spectral fits further justify our adopted spectral models of 2 and 10 MK. Formally they may allow for the possibility of significant circumstellar columns above the expected intervening values, but the constraints are very weak. Cool post-AGB wind material may indeed surround dCs, but such an intriguing possibility must be investigated with much more sensitive X-ray and/or sub-millimeter observations (e.g., Bujarrabal et al. 2013) before being taken seriously.



(a) Counts spectrum



(b) Best-fit X-ray spectral parameters

Figure 5. *Chandra* spectrum of SDSS J125017.9+252427.6 from ObsID 2976. (a) The photon spectrum in counts $\text{ksec}^{-1} \text{keV}^{-1}$. The expected counts for the best-fit $\sim 1\text{MK}$ APEC model is overplotted in red. (b) As in Fig 4, the APEC spectral fit parameter contours of temperature T_X and intervening hydrogen column N_H . The best-fit temperature is near $\sim 1\text{MK}$, but requires an intervening column density much larger than expected from the ISM, broadly consistent with possible circumstellar material.

REFERENCES

- Abate, C., Pols, O. R., & Stancliffe, R. J. 2018, *A&Ap*, 620, A63.
- Afşar, M., & Ibanoglu, C. 2008, *MNRAS*, 391, 802.
- Alam, S. et al. 2015, *The Astrophysical Journal Supplement Series*, 219, 12
- Astropy Collaboration, Price-Whelan, A. M., Sipőcz, B. M., et al. 2018, *AJ*, 156, 123.
- Bailer-Jones, C. A. L., Rybizki, J., Fouesneau, M., et al. 2018, *AJ*, 156, 58.
- Balick, B., & Frank, A. 2002, *ARAA*, 40, 439
- Balick, B. 2004, *AJ*, 127, 2262
- Bilíková, J., Chu, Y.-H., Gruendl, R. A., et al. 2010, *AJ*, 140, 1433
- Blackman, E. G., Frank, A. & Welch, C. 2001, *ApJ*, 546, 288
- Bromm, V., & Loeb, A. 2003, *Nature*, 425, 812
- Bujarrabal, V., Alcolea, J., Van Winckel, H., et al. 2013, *A&Ap*, 557, A104.
- Chabrier, G. & Baraffe, I. 1997, *A&Ap*, 327, 1039.
- Chen, Z., Blackman, E. G., Nordhaus, J., Frank, A. & Carroll-Nellenback, J. 2018, *MNRAS*, 473, 747
- Corradi, R. L. M., Sabin, L., Miszalski, B., et al. 2011, *MNRAS*, 410, 1349
- Cutri, R. M. et al. 2013, *VizieR Online Data Catalog*, II/328
- Dahn, C. C., Liebert, J., Kron, R. G., Spinrad, H., & Hintzen, P. M. 1977, *ApJ*, 216, 757
- Dearborn, D. S. P., Liebert, J., Aaronson, M., et al. 1986, *ApJ*, 300, 314
- de Kool, M. & Green, P. J. 1995, *ApJ*, 449, 236
- Downes, R. A., Margon, B., Anderson, S. F., et al. 2004, *AJ*, 127, 2838
- Evans, I. N., et al. 2010, *ApJS*, 189, 37
- Farihi, J., Arendt, A. R., Machado, H. S., & Whitehouse, L. J. 2018, *MNRAS*, 477, 3801
- Filippazzo, J. C.; Rice, E. L.; Faherty, J.; Cruz, K. L.; Van Gordon, M. M.; Looper, D. L. 2015, *ApJ*, 810, 158
- Fortney, J. J. 2012, *ApJ*, 747, L27.
- Frew, D. J. 2008, Ph.D. Thesis
- Gaia Collaboration, Brown, A. G. A., Vallenari, A., et al. 2018, *arXiv:1804.09365*
- García-Segura, G., Ricker, P. M., & Taam, R. E. 2018, *ApJ*, 860, 19
- Garraffo, C., Drake, J. J., Alvarado-Gomez, J. D., et al. 2018, *ApJ*, 868, 60.
- Gondoin, P. 2018, *A&Ap*, 616, A154
- Green, P. J., Margon, B., & MacConnell, D. J. 1991, *ApJL*, 380, L31
- Green, P. 2013, *ApJ*, 765, 12
- Green, G. M. 2018, *Journal of Open Source Software*, 3(26), 695
- Heber, U., Bade, N., Jordan, S., & Voges, W. 1993, *A&Ap*, 267, L31
- Iaconi, R., De Marco, O., Passy, J.-C., et al. 2018, *MNRAS*, 477, 2349.
- Jeffries, R. D., & Stevens, I. R. 1996, *MNRAS*, 279, 180
- Ji, W., Cui, W., Liu, C., et al. 2016, *ApJS*, 226, 1
- Jones, D., Boffin, H. M. J., Rodríguez-Gil, P., et al. 2015, *A&Ap*, 580, A19
- Jones, D., Van Winckel, H., Aller, A., Exter, K., & De Marco, O. 2017, *A&Ap*, 600, L9
- Kastner, J. H., Montez, R., Balick, B., et al. 2012, *AJ*, 144, 58.
- Kosovichev, A. G., de Gouveia Dal Pino, E., & Yan, Y. 2013, *Solar and Astrophysical Dynamamos and Magnetic Activity*.
- Kraft, R. P. 1967, *ApJ*, 150, 551.
- Li, Y.-B., Luo, A.-L., Du, C.-D., et al. 2018, *ApJS*, 234, 31
- Liebert, J., Schmidt, G. D., Lesser, M., et al. 1994, *ApJ*, 421, 733
- Lucatello, S., Tsangarides, S., Beers, T. C., Carretta, E., Gratton, R. G., & Ryan, S. G. 2005, *ApJ*, 625, 825
- Maldonado, J., Scandariato, G., Stelzer, B., et al. 2017, *A&Ap*, 598, A27
- Margon, B., Kupfer, T., Burdge, K., et al. 2018, *ApJL*, 856, L2
- Matt, S. P., Brun, A. S., Baraffe, I., et al. 2015, *ApJ*, 799, L23.
- Barrett, P., Hunter, J., Miller, J. T., et al. 2005, *Astronomical Data Analysis Software and Systems XIV*, 91.
- Micela, G., Sciortino, S., Serio, S., et al. 1985, *ApJ*, 292, 172
- Miszalski, B., Acker, A., Moffat, A. F. J., et al. 2009, *A&Ap*, 496, 813
- Miszalski, B., Boffin, H. M. J., Frew, D. J., et al. 2012, *MNRAS*, 419, 39
- Miszalski, B., Boffin, H. M. J., & Corradi, R. L. M. 2013, *MNRAS*, 428, L39
- Miszalski, B., Boffin, H. M. J., Jones, D., et al. 2013, *MNRAS*, 436, 3068.
- Miszalski, B., Manick, R., Mikołajewska, J., et al. 2018, *MNRAS*, 473, 2275
- Miszalski, B., Manick, R., Van Winckel, H., et al. 2019, *PASA*, 36, e018.
- Montez, R., De Marco, O., Kastner, J. H., et al. 2010, *ApJ*, 721, 1820.
- Montez, R., Jr., Kastner, J. H., Balick, B., et al. 2015, *ApJ*, 800, 8

- Morales, J. C., Ribas, I., & Jordi, C. 2008, *A&Ap*, 478, 507
- Morgan, D. P., West, A. A., Garcés, A., et al. 2012, *AJ*, 144, 93
- Morrison, R., & McCammon, D. 1983, *ApJ*, 270, 119
- Munn, J. A., Monet, D. G., Levine, S. E., et al. 2004, *AJ*, 127, 3034
- Norris, J. E., Yong, D., Bessell, M. S., et al. 2013, *ApJ*, 762, 28
- Noyes, R. W., Hartmann, L. W., Baliunas, S. L., Duncan, D. K., & Vaughan, A. H. 1984, *ApJ*, 279, 763
- Nutzman, P., & Charbonneau, D. 2008, *PASP*, 120, 317
- O'Dwyer, I. J., Chu, Y.-H., Gruendl, R. A., et al. 2003, *AJ*, 125, 2239
- Oliphant, T. E. 2006, <http://www.tramy.us/>
- Oomen, G.-M., Van Winckel, H., Pols, O., et al. 2018, *A&Ap*, 620, A85
- Pallavicini, R., Golub, L., Rosner, R., et al. 1981, *ApJ*, 248, 279
- Reiners, A., Joshi, N., & Goldman, B. 2012, *AJ*, 143, 93.
- Smith R. K., Brickhouse N. S., Liedahl D. A., Raymond J. C., 2001, *ApJ*, 556, L91
<https://heasarc.gsfc.nasa.gov/xanadu/xspec/manual/XSmodelApec.html>
- Parker, E. N. 1955, *ApJ*, 122, 293
- Plez, B., & Cohen, J. G. 2005, *A&Ap*, 434, 1117
- Reichardt, T. A., De Marco, O., Iaconi, R., et al. 2019, *MNRAS*, 484, 631.
- Ricker, G. R., Winn, J. N., Vanderspek, R., et al. 2015, *Journal of Astronomical Telescopes, Instruments, and Systems*, 1, 14003.
- Rosen, S. R., Webb, N. A., Watson, M. G., et al. 2016, *A&Ap*, 590, A1
- Roulston, B. R., Green, P. J., Ruan, J. J., et al. 2019, *ApJ*, 877, 44.
- Si, J., Luo, A., Li, Y., et al. 2014, *Science China Physics, Mechanics, and Astronomy*, 57, 176
- Skrutskie, M. F.; Cutri, R. M.; Stiening, R.; Weinberg, M. D.; Schneider, S.; Carpenter, J. M.; Beichman, C.; Capps, R.; Chester, T.; Elias, J.; Huchra, J.; Liebert, J.; Lonsdale, C.; Monet, D. G.; Price, S.; Seitzer, P.; Jarrett, T.; Kirkpatrick, J. D.; Gizis, J. E.; Howard, E.; Evans, T.; Fowler, J.; Fullmer, L.; Hurt, R.; Light, R.; Kopan, E. L.; Marsh, K. A.; McCallon, H. L.; Tam, R.; Van Dyk, S.; Wheelock, S. 2006, *AJ*, 131, 1163
- Skumanich, A. 1972, *ApJ*, 171, 565
- Smith, M. C., et al. 2007, *MNRAS*, 379, 755
- Soker, N., & Kastner, J. H. 2002, *ApJ*, 570, 245
- Starkenburg, E., Shetrone, M. D., McConnachie, A. W., et al. 2014, *MNRAS*, 441, 1217
- Stelzer, B., Marino, A., Micela, G., et al. 2013, *MNRAS*, 431, 2063
- Stelzer, B., Damasso, M., Scholz, A., Matt, S.P. 2016, *MNRAS*, 431, 2063
- Tielens, A. G. G. M. 2005, *The Physics and Chemistry of the Interstellar Medium*.
- Testa, P., Drake, J. J., & Peres, G. 2004, *ApJ*, 617, 508.
- Tyndall, A. A., Jones, D., Boffin, H. M. J., et al. 2014, *Revista Mexicana De Astronomia Y Astrofisica Conference Series*, 60.
- West, A. A., Hawley, S. L., Bochanski, J. J., et al. 2008, *AJ*, 135, 785
- Whitehouse, L. J., Farihi, J., Green, P. J., Wilson, T.G., & Subasavage, J.P. 2018, *MNRAS*, 479, 3873
- Wood, P. R., Olivier, E. A., & Kawaler, S. D. 2004, *ApJ*, 604, 800
- Wright, N. J., Drake, J. J., & Civano, F. 2010, *ApJ*, 725, 480.
- Wright, N. J., Drake, J. J., Mamajek, E. E., & Henry, G. W. 2011, *ApJ*, 743, 48
- Wright, N. J., Newton, E. R., Williams, P. K. G., Drake, J. J., & Yadav, R. K. 2018, *MNRAS*, 479, 2351
- Yoon, J., Beers, T. C., Placco, V. M., et al. 2016, *ApJ*, 833, 20